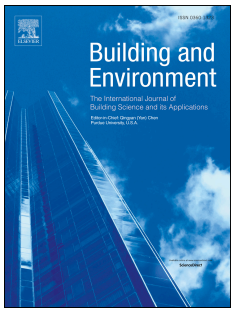

Comparison of different frost models with hygrothermal simulations to better understand frost damage in porous building materials

Kaat Janssens, Chi Feng, Valentina Marincioni, Nathan Van Den Bossche

PII: S0360-1323(24)00241-5

DOI: https://doi.org/10.1016/j.buildenv.2024.111399

Reference: BAE 111399

To appear in: *Building and Environment*

Received Date: 23 November 2023

Revised Date: 5 March 2024

Accepted Date: 9 March 2024

Please cite this article as: Janssens K, Feng C, Marincioni V, Van Den Bossche N, Comparison of different frost models with hygrothermal simulations to better understand frost damage in porous building materials, *Building and Environment* (2024), doi: https://doi.org/10.1016/j.buildenv.2024.111399.

Comparison of different frost models with hygrothermal simulations to better understand frost damage in porous building materials

Kaat Janssens[1*], Chi Feng[2], Valentina Marincioni[3] and Nathan Van Den Bossche[1]

[1]Faculty of Engineering and Architecture, Ghent University, Sint-Pietersnieuwsstraat 41, 9000 Ghent, Belgium

*Corresponding author: Kaat.Janssens@ugent.be

[2]School of Architecture and Urban Planning, Chongqing University, 400045 Chongqing, China

[3]The Bartlett School of Environment, Energy and Resources, University College London, London, United Kingdom

Abstract. Frost damage is one of the most important degradation phenomena of brick facades. Evaluating the risk of frost damage in advance is of utmost importance considering the difficulty of repairing frost damage without replacing the materials, which may not be an option for protected heritage facades. Various performance criteria and methods have been developed over the past decades to assess the risk of frost damage. However, these methods are derived from frost tests under extreme conditions, such as high saturation levels and very low freezing temperatures, and do not represent realistic conditions for mild climates. In 2019, Feng et al. tested four different bricks under milder conditions to understand the relationship of frost damage with freezing temperature and saturation degree. The research in this paper combines the results of Feng's study with hygrothermal simulations, which prove to be a valuable tool for assessing the risk of deterioration of facades of masonry buildings. In this paper, the frost decay assessment methods like the Fc-index, GC-factor and counting the critical

freeze-thaw cycles are examined, discussed and finally dismissed. Finally, a more representative frost decay risk assessment method is proposed.

Keywords: *Frost damage, hygrothermal simulations, freeze-thaw, HAM, facade degradation, risk assessment*

1. Introduction

Frost damage is known to be one of the main causes of deterioration in masonry facades in a moderate climate. A major cause of increased risk of frost damage is a change in the hygrothermal behaviour of the wall. This can be triggered by a changing climate as addressed in literature [1, 2, 3] or by modifying the existing facade. In particular, if the facade has to be retrofitted internally to improve the energy efficiency of a building of high heritage significance, this will drastically change the hygrothermal behaviour through lower drying potential and lower temperatures. Frost damage in a porous medium is the result of ice crystal growth generating a pressure on the internal surface of the pore. When this crystal pressure is higher than the tensile strength of the material, damage occurs [4].

In literature, it can be found that frost resistance of a brick strongly depends on its porosity, tensile strength and pore size distribution [1]. Moreover, Maage et al. developed a correlation between pore characteristics and frost resistance [5]. Of course, it is not only the material properties that pose a risk in frost damage, but also the wall construction and boundary and climatic conditions, which are extremely relevant regarding frost damage. Therefore, Heat-, Air- and Moisture simulations are found to be valuable tools to assess the hygrothermal behaviour of actual wall structures and to gain insights about deterioration risks, because they

can simulate the actual behaviour of the building fabric in relation to dynamic boundary conditions. HAM-tools, like WUFI and Delphin, are often used to evaluate moisture-related risks.

Using data from these tools, different approaches are found in literature to assess the risk of frost damage. Very often in practice, the number of normal freeze-thaw cycles (FTC) is quantified by counting the number of times the temperature drops below the 0°C threshold . However, this does not take into account the freezing-point depression phenomenon: at temperatures below 0°C, water freezes in larger pores first. Water requires lower temperatures to freeze in smaller pores in order to lead to damage, due to an increase in capillary pressure as the pores become smaller. Besides building sciences, valuable research is conducted on the cause of damage due to ice growth in the research fields of geomorphology, physics and material sciences. Geomorphology studies argue that frost damage is not a consequence of the 9% volume expansion of ice to which it is usually attributed. However, frost damage is usually a consequence of cryosuction, which is the flow of fluid into a frozen area of ice crystals that fuels ice growth [6, 7]. This flux is significant and ongoing when ice formation takes place. Further, Wettlaufer et al. [8] discusses that the net force on the pore walls is not due to capillarity itself, but caused by the intermolecular forces that produce interfacially premelted films.

Freezing temperatures do not necessarily induce damage in a porous material, the combination of moisture content and the degree of saturation are the important factors that affect the actual damage risk [9]. This is supported by research of Fagerlund et al. who developed the critical degree of saturation method to assess freeze-thaw resistance of concrete [10]. The critical degree of saturation (S_{crit}) is used as a threshold moisture level to prevent frost weathering. Next, Prick

et al. [11] examined the S_{crit} of ten limestones from France and reported that this was between 0.58 and 1.0. Mensinga et al. [12] reported that the S_{crit} for three Canadian bricks varied between 0.25 and 0.87. Therefore, the method of counting critical freeze-thaw cycles (FTC_{crit}) was developed: one FTC_{crit} is counted when the ice mass volume over the pore volume surpasses a certain value. Often the threshold of 25% is adopted as a conservative approach as this is the lowest S_{crit} reported in literature. This 25% criterion should be better for comparative studies rather than the often assumed 91% criterion taking into account a 9% ice expansion due to freezing [6, 13]. A lower threshold value leads to a higher number of cycles, and reduces the risk that very small changes in hygrothermal behaviour are misinterpreted. A slight increase in moisture content during one event may lead to an additional FTC: this is significant if the number of FTC rises from 2 to 3, but insignificant when it rises from 20 to 21. However, how many FTC_{crit} result in actual frost damage is unclear.

Furthermore, one major concern arises from the fact that typical freeze-thaw tests on bricks, subjecting samples conditioned to a certain moisture content to alternating freeze-thaw cycles, make use of very high moisture contents and very low freezing temperatures. Specifically, the Belgian standard NBN B 27-009 requires to fully saturate the specimen under vacuum pressure followed by 20 frost cycles to -15°C [14]. Therefore, the test can be regarded as a pass/fail criterion: if a brick shows no damage after such extreme conditions, it will most likely perform well under milder conditions. If it fails, it can be considered as unsafe. Whether these tests are representative for realistic frost conditions in a masonry facade, is of course questionable. Most test standards related to freeze-thaw evaluation were developed for certification of new products, and similarly impose conservative (severe) test conditions. They don't necessarily

perform well as a response-based criterion, since damage could also occur under less extreme conditions. As a reaction, Feng et al. performed freeze-thaw tests on bricks under milder and realistic moisture contents and freezing temperatures [15].

Using the results of hygrothermal simulations in combination with the experimental results of Feng et al, different frost decay assessment methods are evaluated in this paper and future approaches are proposed, with the aim of making improvements in freeze-thaw damage assessments under realistic conditions.

2. Materials and methods

The next part of this paper is divided in 4 sections. First, the needed pore physics theory is explained to understand frost damage in porous media. The second section will look closer at the different methods available in literature and applied methodologies to assess frost damage. The simulation set-up is explained in section 2.3, and the final part describes the assessment method of the simulation results.

2.1 Pore physics theory

The section below describes the equations for coupled moisture and heat transport for a freezing porous medium with a certain temperature T [K]. It is assumed that Kelvin's equation (Eq. 1), which describes the capillary pressure p_c [Pa] as a function of the relative humidity φ, is still valid as liquid water, ice and vapour coexist in the porous medium under freezing conditions. Next to that it is assumed that each phase is in equilibrium with each other. More precisely, p_c is the difference between the air pressure and the liquid pressure along their common interface, which can be expressed as shown in Equation 1.

$$p_c(\varphi) = -\rho_l * R_v * T * \ln \varphi \qquad \textit{Eq. 1}$$

With ρ_l: density of water [kg/m³], R_v: gas constant vapour [J/kgK]

Eq. 2 describes the Young-Laplace equation, which describes the capillary pressure p_c in an unfrozen state with the pore radius r. This shows the correlation between the pore size distribution of a material and its moisture retention curve (MRC) resulting in smaller pores having a higher capillary pressure than larger pores.

$$p_c = \frac{2 * \gamma_{vl} * \cos \alpha}{r} \qquad \textit{Eq. 2}$$

With α: contact angle [°] and γ_{vl}: surface energy of vapour-liquid interface [Jm^{-2}]

The reason that both liquid water and ice coexist in a freezing porous medium is due to the freezing point depression, meaning the freezing temperatures of a liquid in a porous medium are dependent on the pore size, therefore water freezes in smaller pores at temperatures below 0°C. Because the ice formation removes pore water from the system, a gradual ice formation occurs. Therefore, the pore radius of liquid-filled pores r decreases, hence diminishing the temperature at which freezing can take place and the pore water pressure. Eq. 3 shows the relation between the pore radius and freezing point depression [16]:

$$\ln \frac{T}{273.15} = \frac{-2 * v_l * \gamma_{il}}{\Delta h_{ice}} * \frac{1}{r} \qquad \textit{Eq. 3}$$

With v_l: specific volume liquid [m³/mole], γ_{il}: ice-liquid interfacial energy [Jm^{-2}], Δh_{ice}: Average molar heat of melting ice [J/mole]

As discussed in the context of freezing of concrete [17], in the pore a solid-liquid thermodynamic equilibrium is required. This equilibrium between the crystal pressure p_{crys} and the liquid pressure p_l is described in Eq. 4

$$p_{crys} - p_l = \Delta S_{fv}(T_0 - T) \qquad \textit{Eq. 4}$$

With ΔS_{fv}: the entropy of fusion per unit volume of crystal [J/Km³] equals to 1,2 J/cm³K [18], T_0: freezing reference temperature (=273.15 K)

If we want to show the equilibrium of the solid-liquid interface in relation to the pore radius, we can derive Eq.5 from the former equations (i.e. Eq. 3 and Eq. 4), assuming that the contact angle between the ice and the liquid is zero.

$$p_{crys} - p_l = \frac{2 * \gamma_{il}}{r} \qquad \textit{Eq. 5}$$

With γ_{il}: Ice-liquid interfacial energy [Jm^{-2}]

When it freezes, the larger pores freeze first and only when the temperature drops the smaller pores will start to freeze, assuming that the porous media is non-deformable and there is no salt present [9].

Combining the previous equations give the Gibbs-Thomson law (Eq.6) which shows the pore radius of the smallest pore that freezes at a temperature T [9].

$$r = \frac{2 * \gamma_{il}}{\Delta S_{fv} * (T_0 - \mathrm{T})} \qquad \textit{Eq. 6}$$

Pore radius r is the radius of the smallest pore that freezes at temperature T in the porous medium (the water in all pores smaller than r remains liquid). All pores with a radius bigger or equal to r freeze at temperature T. The ice-liquid interfacial energy γ_{il} [Jm^{-2}] is equal to 0.29 Jm^{-2} [19].

Fig. 1 conceptually depicts the ice formation in a porous medium. Starting from the established principles of phase behaviour as described above, we can simply state that when curved phase boundaries occur, there is a pressure difference proportional to the relevant surface energy. Since the surface energy of a vapour-liquid interface is about twice the energy of an ice-liquid interface and the liquid pressure is uniform, an ice-liquid interface can be in equilibrium in pores with a diameter of approximately twice the diameter of pores needed for a vapour-liquid interface equilibrium. This considers vapour pressure in pores staying close to atmospheric pressure (p_{atm}) due to buffering effects. Consequently, with some vapour present, there is little opportunity for overburden to be supported by ice so p_{crys} is also expected to remain close to p_{atm}. Therefore, it is possible to calculate the percentage of frozen pores in the whole pore system using the Moisture Retention Curve (MRC), illustrated by Figure 1. The smaller pores are filled with liquid first (blue zone), but potential freezing of the pores starts from the larger pores to the smaller ones due to freezing point depression (red zone). Naturally, it is only possible to freeze the pores if there is liquid inside. Therefore, only in the overlapping zone (purple zone) it is possible to have pores filled with ice, because only in this pore size fraction is liquid available in the pores to freeze. This could be described as the ice-volume fraction, which is the volume fraction of the pore space filled with ice.

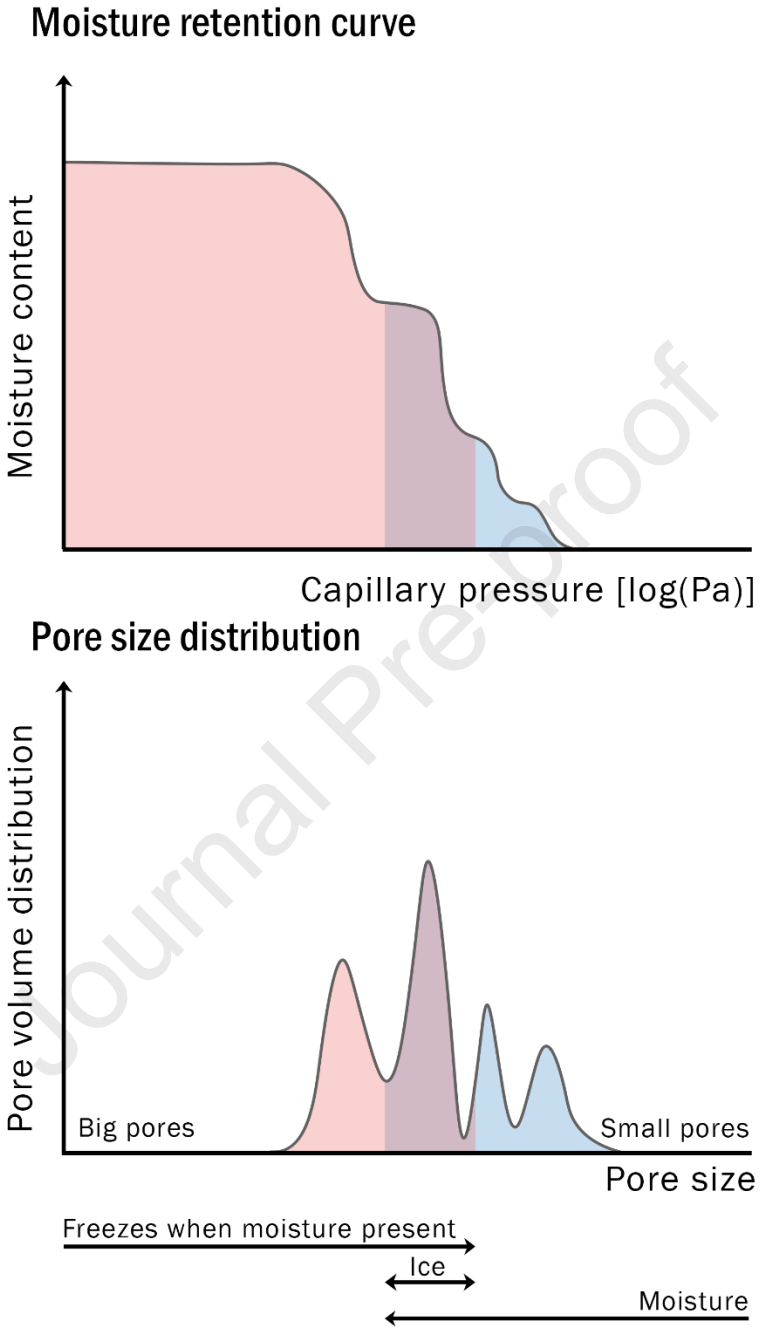

Figure 1: Moisture retention curve and pore size distribution showing in which pores ice can be formed, resulting in the ice-volume fraction.

2.2 Methods frost assessment

Different frost assessment methods are discussed in this section. The first ones, the F_c-index and GC-factor, only consider material sensitivity to frost, thus being solely material-based. The other three assessment methods also include the exposure to a certain climate, thus being exposure-based. When evaluating the output of hygrothermal simulations of a wall set up, the performance criteria methods are calculated for the depth of 5 mm from the exterior surface, shown in literature as the critical depth for frost damage [20, 13], although this has been questioned recently by Prignon et al. who claim a 10 mm depth might be more critical [21]. Since this discussion is out of scope for this paper, the 5mm critical depth approach is assumed.

2.2.1 Material sensitivity: Fc & GC

Two different ways commonly used in Belgium [22, 23] to determine the frost sensitivity of a brick are solely based on material characteristics: the F_c-index (calculated frost resistance number)[-] from Maage et al. [5] and the GC-factor (*Gélivité basée sur Capillarité - in French, translated to English:* frost based on capillarity) [-].

The F_c-index is a well-known index to determine whether a material is frost-resistant or frost-sensitive and is shown in Eq. 7.

$$F_c = \frac{0.0032}{PV} + 2.4 * P_3 = 0.0032 * \frac{\rho_{bulk}}{\varphi} + 2.4 * P_3 \qquad \textit{Eq. 7}$$

With PV: pore volume per unit mass (m^3/kg), P_3: pore volume fraction for pores diameter larger than 3 µm (%)

If $F_c > 70$ the brick is considered frost resistant, if $F_c < 55$ it is classified as frost sensitive, intermediate values translate to an uncertain transition zone. Maage's research is based on lab tests on 13 different types of bricks, 9 from Norway and 4 from USA. A number of methods were applied to correlate pore size distribution characteristics with observed frost decay. It was found that materials having a greater number of large pores, are more resistant to frost damage.

Another material-based approach which is commonly used in Belgium is the GC factor (Eq.8), for which no information about the pore size distribution is needed.

$$GC = -14.53 - 0.309 * \left(100 * \sqrt{60} * \frac{A_{cap}}{w_{sat}}\right) + 0.203 * (100 * \frac{w_{cap}}{w_{sat}}) \qquad \textit{Eq. 8}$$

With A_{cap}: capillary absorption coefficient [kg/m²s$^{0.5}$], w_{sat}: saturated moisture content [kg/m³] and w_{cap}: capillary moisture content [kg/m³]

The GC factor was found based on a correlation between frost resistance of materials and capillary absorption. Based on the GC-value, the level of frost resistance is assigned as described in Dusar et al. [24]. This method was developed for different ceramic materials, the equation above is the one specific for bricks. Values lower than -3.93 are reported to be very frost resistant, -1.50 implies frost resistant, +1.59 medium frost resistant, +2.00 barely frost resistant and values higher than +2.57 are deemed not frost resistant.

2.2.2 Exposure based: Critical freeze thaw cycles

An exposure-based criterion widely applied in research is counting the critical number of freeze-thaw cycles (FTC_{crit}), based on the research of Mensinga et al. [12] The critical degree of moisture saturation (S_{crit}) is assessed for freeze-thaw damage using the frost dilatometry

method. In that study, the brick samples were saturated to different saturation degrees and underwent six cycles of freezing and thawing from -15°C to 20°C. S_{crit} is defined as the lowest saturation level for which the expansion exceeded 100 microstrain. The study was performed for three Canadian masonry bricks; one modern, and two historic bricks. The critical degree of saturation varied between 87% for the modern one and between 25% and 30% for the two historic bricks. In scientific literature analysing freeze-thaw damage, when the number of critical freeze-thaw cycles is counted, the 25% criterion is typically applied ($FTC_{crit}^{0.25}$).

2.2.3 Exposure based: Ice-volume fraction

As mentioned in section 2.1, applying pore physics makes it possible to calculate the ice-volume fraction during exposure. This is the percentage of pores filled with ice over the total open pore structure. Observing the most extreme conditions during a FTC can provide relevant insights in understanding freeze-thaw damage. With this method, every time the material is exposed to a FTC, the highest ice-volume fraction is calculated. Note that this is not an existing exposure based criterion. Nevertheless, it could provide relevant insights since it combines information on both moisture, temperature and material characteristics.

2.2.4 Exposure based: Ω-factor

Calculating the Ω-factor for evaluating the deterioration of bricks due to frost damage is a method used in the study of Chi Feng et al. [15, 25]. The study was based on the argument that standard freeze-thaw tests are not representative as these are done for very low freezing temperatures and very high saturation degrees; as these were designed as conservative pass/fail test for new materials instead of response assessment. In many climates, these conditions are

not likely to occur throughout the expected service life. The study performed FTC for 4 different bricks; A, B, C and D, for different freezing temperatures and saturation degrees, as reported in Table 1. Brick A is stated to be a frost-resistant brick, while B is frost-sensitive. Bricks C and D were produced for the project with different firing temperatures, of 925 and 970°C respectively.

Brick type	T= -2°C	-4°C	-6°C	-8°C	-14°C	-20°C
S= 0.10	-	-	-	-	-	A,B,C,D
0.25	B	B	B	B	B	A,B,C,D
0.40	B	B	B	B	B	A,B,C,D
0.55	A,B,C,D	A,B,C,D	A,B,C,D	A,B,C,D	A,B,C,D	A,B,C,D
0.70~0.75	A,B,C,D	A,B,C,D	A,B,C,D	A,B,C,D	A,B,C,D	A,B,C,D
0.85	A,B,C,D	A,B,C,D	A,B,C,D	A,B,C,D	A,B,C,D	A,B,C,D
1.0	A,B,C,D	A,B,C,D	A,B,C,D	A,B,C,D	A,B,C,D	A,B,C,D

Table 1. Test conditions for the different brick types. With S: saturation degree [-] (Feng C. et al. 2019)

After 5 and 10 frost cycles the frost damage was evaluated using ultrasonic testing. The test applies an ultrasonic pulse from one transduces to the other recording by t_0 and t [s] as the time needed for the pulse to travel across the sample. By doing so, the Young's moduli E [Pa] of the samples were obtained and the relative change of the dynamic elasticity modulus, or Ω-factor, was derived following Eq. 9 [25].

$$\Omega = 1 - \frac{E}{E_0} = 1 - \left(\frac{t_0}{t}\right)^2 \qquad \textit{Eq. 9}$$

With E and E_0: elasticity moduli [Pa] before and after freeze-thaw cycling, t and t_0: time t [s]

This method was applied for both 5 and 10 freeze-thaw cycles resulting in $\Omega^{5\ cycles}$ and $\Omega^{10\ cycles}$. A major advantage of the Ω-factor is that it has a clear threshold value for frost damage described in EN 12371:2010 [26]. If the relative change of the dynamic elasticity modulus

surpasses 30% (Ω-factor>0.3), the brick has already one or several cracks larger than 0.1 mm width or detachment of fragments larger than 30mm² per fragment. Therefore, a Ω-factor of 0.3 is often adopted in practice as threshold value.

In this paper, this threshold is used within a response –based method. For each freeze-thaw event, the most extreme combination of freezing temperature and corresponding saturation degree is recorded as a single value. Subsequently, the Ω-factor is assigned for each level of frost occurrence derived from the results of Feng et al. [15] shown in Eq. 10.

$$\Omega = \begin{cases} \dfrac{\Omega^{5\ cycles}}{5} * x, & x \leq 5\ cycles \\ \Omega^{5cycles} + \dfrac{\Omega^{10\ cycles}}{10} * (x-5), & x > 5\ cycles \\ \Omega^{10\ cycles}, & x > 10\ cycles \end{cases} \quad \textit{Eq. 10}$$

With x: number of FTC for the combination of saturation degree and freezing temperature compartmentalised as in Table 1

In literature it is often explicitly or implicitly assumed that an increase in the number of cycles leads to more frost damage. However, other research shows the exponential reduction of the impact of the number of frost cycles on the frost damage quantified with Ω [15, 27, 28]. This is confirmed in the research of Feng et al. (2019): the damage increase from $\Omega^{5\ cycles}$ to $\Omega^{10\ cycles}$ can be considered insignificant. Therefore, as only Ω-factors for 5 and 10 cycles are available, the number of cycles is split into an impact lower than 5 cycles and more than 5 cycles with the $\Omega_{10\ cycles}$ as a maximum value, to take into account the diminishing value of Ω for a higher number of cycles.

2.3 Simulation set-up

To quantify the response-based methods for frost assessment as discussed in section 2.2, the results of hygrothermal simulations are applied. In the next section, the set-up of these simulations is explained. HAM-simulations provide the opportunity to gain insights into the hygrothermal and dynamic behaviour of a wall and its materials in a realistic setting with changing boundary conditions without expensive and time-consuming experimental work. Therefore, different solid wall configurations were simulated, while varying geometry, material properties and boundary conditions based on Calle et al. [13]. The different parameter combinations can be found in Table 2. Every combination of parameters was simulated (full factorial, i.e. 41472 simulations) in the software Delphin 6.1. The reader can, next to the information provided in the paragraph below, refer to the manual of the Delphin software to find more information about the set-up of a Delphin model [29]. The set-up was done using 1D simulations to limit the computational expense. Because of the use of the 1D simulations the impact of mortar joints and other non-1D wall properties such as heterogeneous material characteristics, deficiencies, or wooden beam heads embedded in a wall were not taken into consideration. Please refer to [30] for a more detailed discussion on the differences between 1D and 2D modelling. For the comparative assessment of freeze-thaw criteria for brick material focusing on the interaction between boundary conditions and material properties, the 1D approximation does not introduce a systematic bias.

Parameter	Variations	Description
Climate	4	Historical climate (1972-2005), Climate projections RCP 2.6, RCP 4.5 and RCP 8.5 (2066-2099)
Orientation	8	N, N-E, E, S-E, S, S-W, W and N-W
Wall thickness	3	150 mm, 300 mm and 450 mm
Brick	4	ZH, ZG, ZB and ZK
Insulation type	3	None, vapour open and capillary active insulation
Insulation thickness	3	50 mm, 100 mm and 150 mm
Rain exposure coefficient	4	0.5, 1.0, 1.5 and 2 [-]
Shortwave exposure coefficient	3	0.4, 0.6 and 0.8 [-]

Table 2. Parameter variation for the hygrothermal simulations

2.3.1 Material data

When applying the Ω-factor method with results from hygrothermal simulations, bricks A, B, C and D from the study of Feng et al. [15] need to be linked to a representative material from the material database of Delphin, as the bricks A, B, C and D are not fully characterised to enable direct implementation in hygrothermal modelling. The bricks from the experimental study of Feng et al. and the existing bricks from the Delphin material database were first put together into one dataset and then clustered based on their physical properties known (w_{sat}, w_{cap} and A_{cap}) [31]. The clustering method applied here is the Ward method, reported to be the most robust clustering method [32]. The results are depicted in Figure 2.

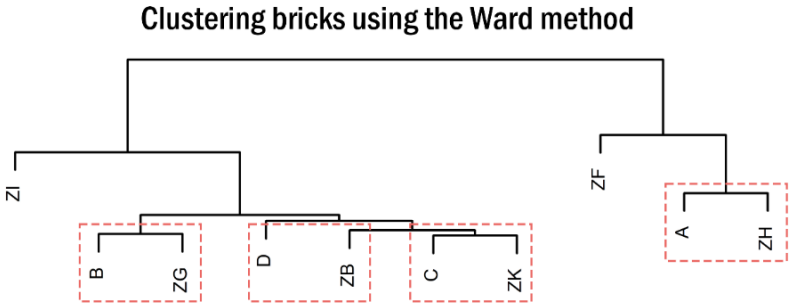

Figure 2. Clustering results using the Ward method

Furthermore, two different interior insulation systems were modelled: a vapour-open system with a vapour control layer (VCL) of s_d=2.3m and a capillary active system represented by calcium silicate without a vapour barrier.

2.3.2 Climate

The climate data consists out of 30-year climate data from the ALARO-0 Regional Climate Model [33], [34] for the grid point of Brussels, Belgium. To take the impact of climate change into account, three different representative concentration pathways (RCP's) were considered as described by Vandemeulebroucke, et al. (2023) [35], namely RCP 2.6, RCP 4.5 and RCP 8.5. The RCP index equals the radiative forcing [W/m²]. These RCP scenarios can be considered as a strong mitigation scenario, a moderate one and a very high emission scenario respectively. The historical climate data period refers to 1976-2005, whereas the climate projections cover the period 2066-2099.

2.3.3 Boundary conditions

Heat and water vapour transfer coefficients at the exterior surface depend on wind velocity, for which EN ISO 6946 was consulted [36]. The hourly Wind-Driven Rain (WDR) intensity is derived following EN ISO 15927-3 [37]. Furthermore, the shortwave absorption coefficient of the building surface is varied between 0.4, 0.6 and 0.8 taking into account the colour of different facade finishes. The values for the albedo of the ground surface and the longwave emission coefficient of the building are fixed at respectively 0.2 and 0.9. Four different rain exposure coefficients were adopted as evident from Table 1, to integrate the effect of different surroundings, wall factors, runoff, malfunctioning gutters and roof overhangs, namely 0.5, 1,

1.5 and 2 [38], [39]. Because the wall orientation is one of the most influential parameters regarding freeze-thaw damage [40], 8 different orientations were included.

2.4 Methodology analysis

As the Ω-factor provides a clear and measurable decay index, it is assumed that the Ω-factor is the most realistic and reliable reference. Furthermore, the different combinations of freezing temperatures and saturation degrees are more representative for the temperate maritime climates considered in this study. Moreover, this method benefits from having a clear threshold value for damage when Ω>0.3. Accordingly, a comparison will be made between this Ω-factor method and the other methods to identify which approaches are most representative to assess the risk of frost damage.

3. Results and discussion

This section comprises three parts. First, the assessment of freeze-thaw damage criteria is discussed for a single combination of parameters to demonstrate the workflow and interpretation of results in section 3.1. Secondly, the entire dataset of 41.472 simulations is examined to evaluate whether the conclusions from the single configuration are valid for all configurations in section 3.2. Finally, the paper examines ways to improve overall freeze-thaw damage prediction with the results of this study in section 3.3.

3.1 Reference case

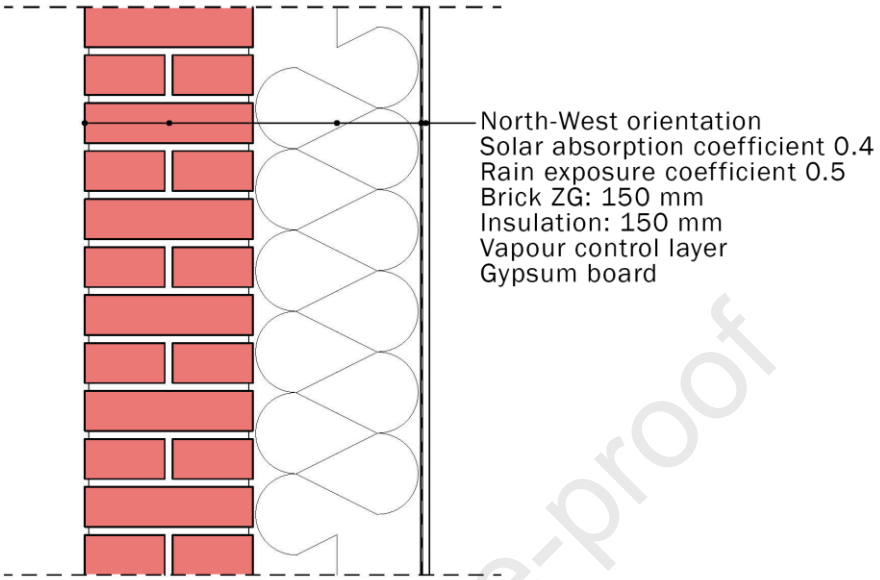

Figure 3. Wall configuration reference case

Figure 3 provides an overview of the reference case which will be discussed in this section. In Table 3. the reader can find a 1-year average for the reference case of the different FTC based on the hourly output of the simulations, their representative values and how an overall Ω-factor was derived for this case. It is clear that a high number of FTC does not necessarily correspond to a high Ω-factor, since for this case only the FTC to -8.2°C with a saturation of 0.2 entails an Ω-factor above zero as a result. This also illustrates that a certain FTC does not have to happen often to result in long-lasting damage.

FTC- category	Number of FTC	Representative temperature	Corresponding saturation	Ω-factor
< -2°C	19.6	-2.20°C	0.14	0.00
< -4°C	7.6	-4.21°C	0.15	0.00
< -6°C	3	-6.19°C	0.14	0.00
< -8°C	1.8	-8.20°C	0.20	0.049
				Ω: 0.049

Table 3. Reference case of FTC and corresponding values for 1 year-average, facilitating a comparative analysis

Table 4 on the other hand, summarises the results for the different methods of frost assessment for this reference case. The different results all provide a different appreciation of the frost damage risk. The low GC-factor found here indicates the material is expected to be frost resistant. The same conclusion is valid for the F_c-index (note that the higher this factor, the more frost resistant the material is). Looking at the low number of $FTC_{crit}^{0.25}$, it can be concluded that a low risk of frost damage is expected. However, if the Ω-factor is taken into consideration, severe frost damage is expected in 10 years (this example shows the average 1 year results). This high Ω-factor is the result of a cycle with a very low freezing temperature and a relatively high saturation as evident from Table 3.

Frost assessment method	Value	Implication
F_c-index	161.1	Frost resistant
GC-value	-1.5	Frost resistant
$FTC_{crit}^{0.25}$	1.8	Low number of critical frost cycles
Maximum ice-volume fraction	11.6 %	Unknown
Ω	0.049	Severe frost damage in 10 years

Table 4. Reference case results different frost assessment methods for 1 year average

Under the assumption that Ω-factor is most reliable because it is based on experimental results and takes into account different freezing temperatures and moisture contents, it can be stated that not all performance criteria entail a trustworthy result. On the one hand, this is because the

F_c-index and GC-factor do not take into account the actual response of materials enduring realistic climate conditions. On the other hand, the method of counting $FTC_{crit}^{0.25}$ is based on experimental results under very extreme conditions and does not consider cycles to milder freezing temperatures and lower saturation degrees, which are far more realistic to occur outside laboratory conditions in temperate maritime climates.

3.2 Whole dataset

In this part, we investigate whether the conclusions derived from a single case are also valid for the whole dataset. First, the performance of the material sensitivity methods represented by the F_c-index and GC-factor is evaluated. Secondly, the conditions during a FTC are discussed. Lastly, the $FTC_{crit}^{0.25}$ method is questioned when compared with the results of the Ω-factor.

3.2.1 *Ω versus F_c and GC*

Figure 4 shows the Ω-factor plotted against the F_c-index and the GC-factor. A decreasing trend would be expected when looking at the F_c-index and the corresponding Ω-factor because the higher the F_c-index, the more frost resistant the material should be. Nevertheless, looking at the whole dataset, the two indices do not agree. Likewise, an increasing trend should appear for the GC-value, since the lower this factor the more frost resistance the material is expected to be. However, the opposite trend shows when plotted in correlation with the Ω-factor. It can be concluded that the F_c- and the GC-factor are not representative risk assessment methods under realistic conditions. Using the F_c-index and the GC-factor as reliable frost decay risk assessment factors is hereby rejected.

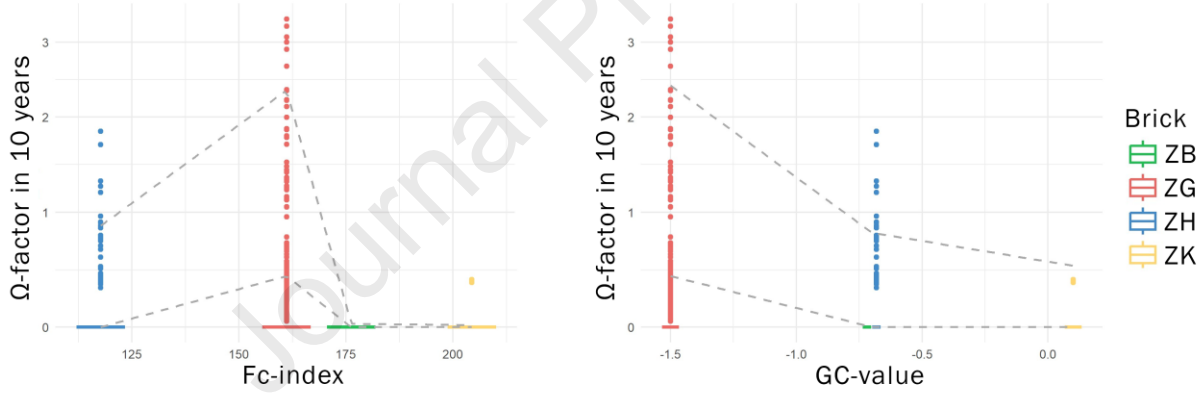

Figure 4. Fc-value and GC value plotted in relation to the Ω-factor in 10 years. The dotted lines connect the 97.72nd and 99.87th percentile.

3.2.2 *Ω and FTC conditions*

First, the impact of different parameters during freeze-thaw events on the Ω-factor is studied. The spearman rank correlation (Rho) between saturation, freezing temperature and ice-volume fraction when a FTC occurs is illustrated in Figure 5. For comparison, also the number of

$FTC_{crit}^{0.25}$ is shown. The higher the Rho-factor is, the more strongly the Ω-factor is correlated with the examined variables.

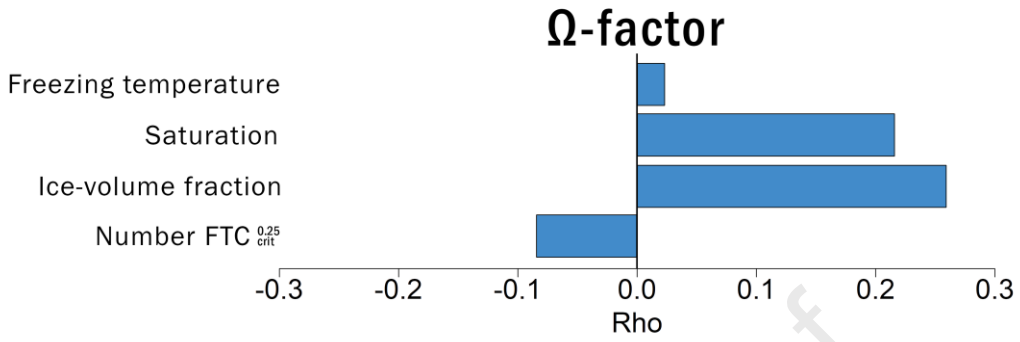

Figure 5: Spearman rank correlation with the rho-value for the impact of different conditions during a FTC.

Instinctively, an equally high correlation is expected between the Ω-factor withthe freezing temperature and saturation degree because the Ω-factor results from the combination of the two. However, in Figure 5 it becomes clear that the saturation degree is far more significant than the freezing temperature. This proves that looking at temperature only is by no means sufficient to assess frost damage. Next to that, the ice-volume fraction during the FTC has the highest correlation with the Ω-factor, which proves the ice-volume fraction to be of great value since this combines information on both moisture, temperature as material characteristics.

Furthermore, it is striking to find that the number of $FTC_{crit}^{0.25}$ is correlated negatively with the Ω-factor. This is counterintuitive, and clearly undermines the idea that the more critical freeze-thaw cycles occur, the more damage is expected. Research showed that the impact of the number of FTC on degradation exponentially decreases as discussed in section 3.2.d.However, finding a negative correlation does require a more in depth elaboration, which is reported in the following part of the paper.

3.2.3 *Ω versus* $FTC_{crit}^{0.25}$

In the single case analysis reported in section 3.1 it already came to front that the $FTC_{crit}^{0.25}$ method yields misleading results compared to the Ω-factor. In Figure 6, the Spearman rank correlation is depicted showing the impact of the wall variables on the number of $FTC_{crit}^{0.25}$ (left) and the Ω-factor (right). It can be seen that the overall trends (positive/negative) remain the same despite differences in magnitude. Only for the influence of the brick type an opposite impact is observed. Due to the material-dependency of the results, the brick type that performs worst at the $FTC_{crit}^{0.25}$ criterium and the Ω method is not the same one.

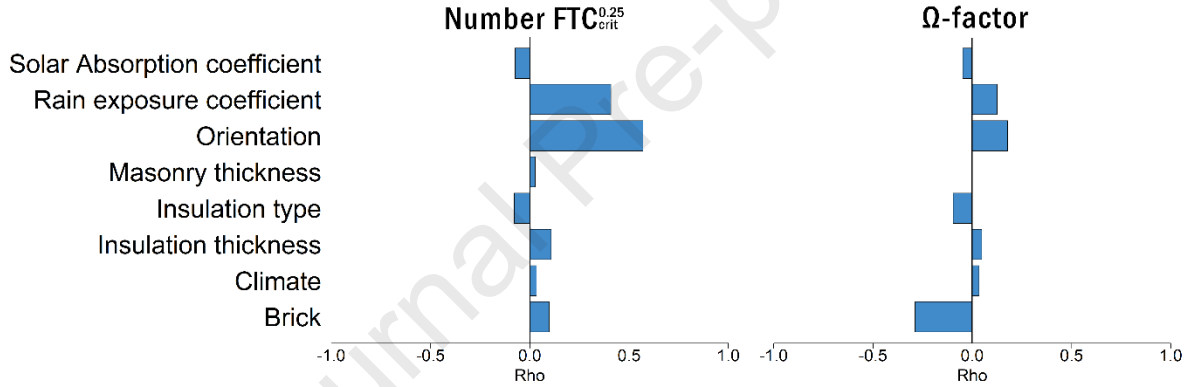

Figure 6. Spearman rank correlation with the rho-value for the impact of the different parameters on the number of $FTC_{crit}^{0.25}$ and the Ω-factor.

A rationale of why the $FTC_{crit}^{0.25}$ method has different outcomes than the Ω-factor method could be that the criterion of 25% is not the right S_{crit} for the simulated bricks. This reasoning is supported by the results from the original research of Mensinga et al. and Prick et al. [11, 12], that found S_{crit} for different bricks ranging from 25% to 87%. It could be possible that a better correlation between both is found when each brick is evaluated using the actual value for S_{crit} (information which is not available) . To examine this hypothesis the number of FTC_{crit}^{X} was

quantified for a variety of S_{crit} going from 5% to 90% with a 5% interval. In Figure 7, the different FTC_{crit}^{X} are shown in correlation with the Ω-factor for each brick .

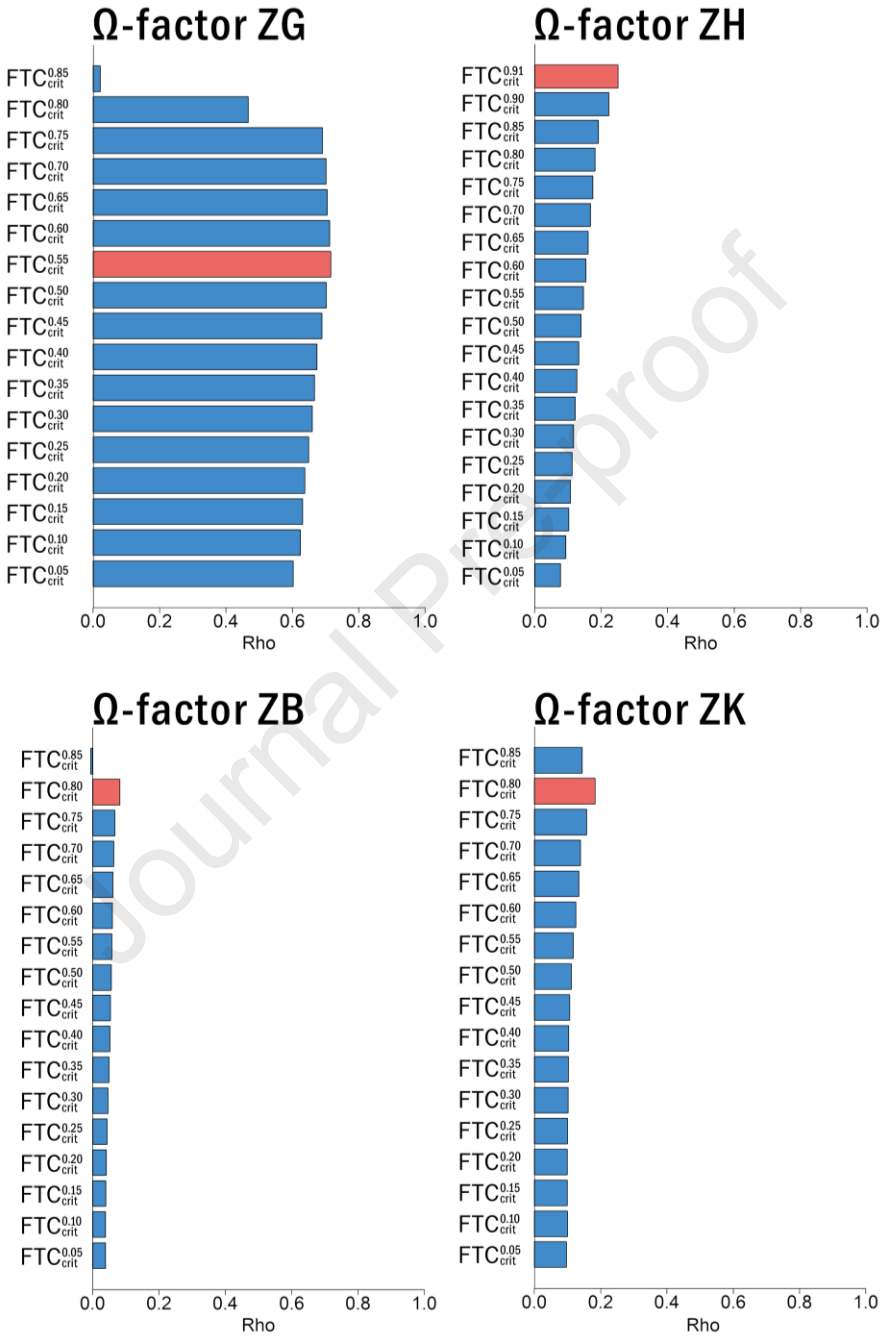

Figure 7: Spearman rank correlation with the rho-value for the impact of the number of FTC_{crit}^{X} for different S_{crit} for the different bricks. Red: highest correlation.

The results show that for different bricks, a different S_{crit} entails the best correlation with the Ω-factor. It is clear that not one critical saturation degree proves to be superior over others considering all bricks. Moreover, if you could measure the S_{crit} for each brick, which is not a simple measure, the influence of this criterion is very material sensitive and result only for some bricks in a valuable correlation. It can be concluded that the FTC_{crit}^{X} method is unreliable and very material dependent to assess frost decay risk.

As was demonstrated clearly in Figure 5, the number $FTC_{crit}^{0.25}$ is negatively correlated with the Ω-factor. The reason becomes clear in Figure 8, in which the number of FTC's for different freezing temperatures is plotted in relation to the mean corresponding saturation degree. Each red dot depicts one FTC. In blue, the trend is plotted with the confidence level in grey. FTC's to -8°C are not depicted, since this event happened too infrequent to draw a clear trend. It highlights that under real climatic conditions, simulated for the historical climate and three climate projections, enduring a large number of FTC's results that the majority of these FTC's occur at a low saturation degree. The saturation degree during a FTC is of high significance for the Ω-factor. Therefore, FTC's with lower saturation do not entail as much damage as FTC's with a higher saturation. As a result, this analysis demonstrates that counting the number of $FTC_{crit}^{0.25}$ to assess damage is an unreliable metric to asses frost damage risk.

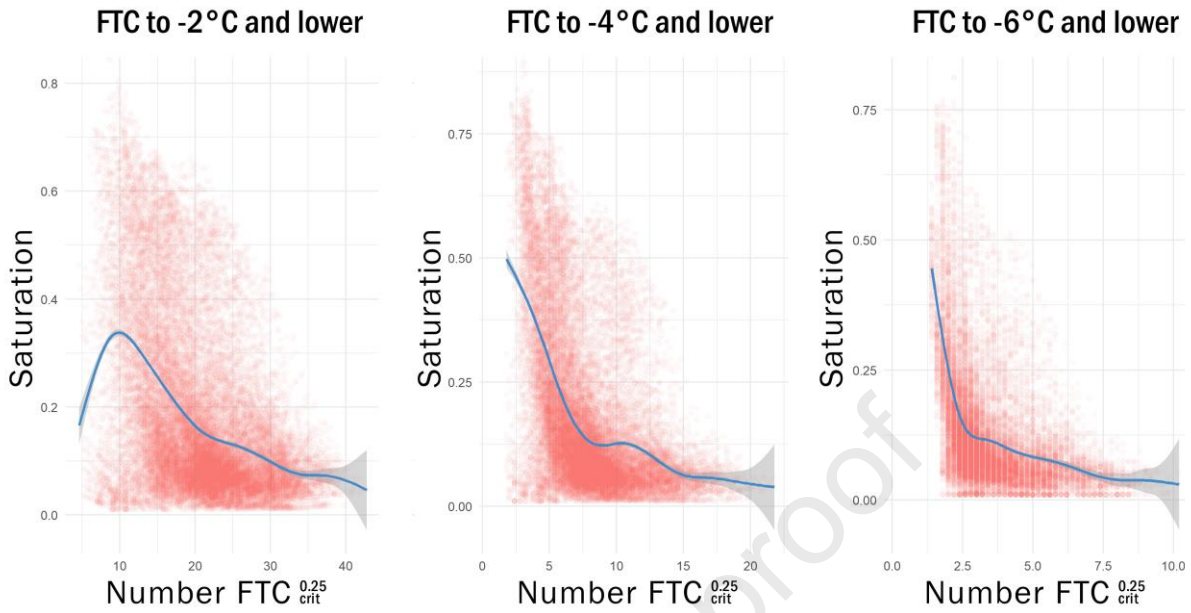

Figure 8: Scatterplot of the number of $FTC_{crit}^{0.25}$ and their corresponding saturation degree.

Given the distinct differences between the various performance criteria, the impact of different wall characteristics on freeze-thaw damage could radically shift. Therefore the next section examines a topic often discussed in literature: the critical orientation for frost damage and its expected future climate behaviour. Figure 9 comprises 4 graphs with detailed results for the different freeze-thaw criteria.

A south-west orientation is generally asssumed to be the critical orientation for frost damage in Belgium being the most critical orientation for wind driven rain. However, plotting the critical orientation for the Ω-factor, the west orientation comes to front. Furthermore, the mean Ω-factor entails frost damage will increase for future projections. The same trend can be seen for the ice-volume fraction and the saturation during a FTC. These results contradict previous findings based on the number of $FTC_{crit}^{0.25}$ stating frost damage is likely to decrease in the future

climate [41]. This proves again, how important it is to study and keep reviewing frost performance criteria.

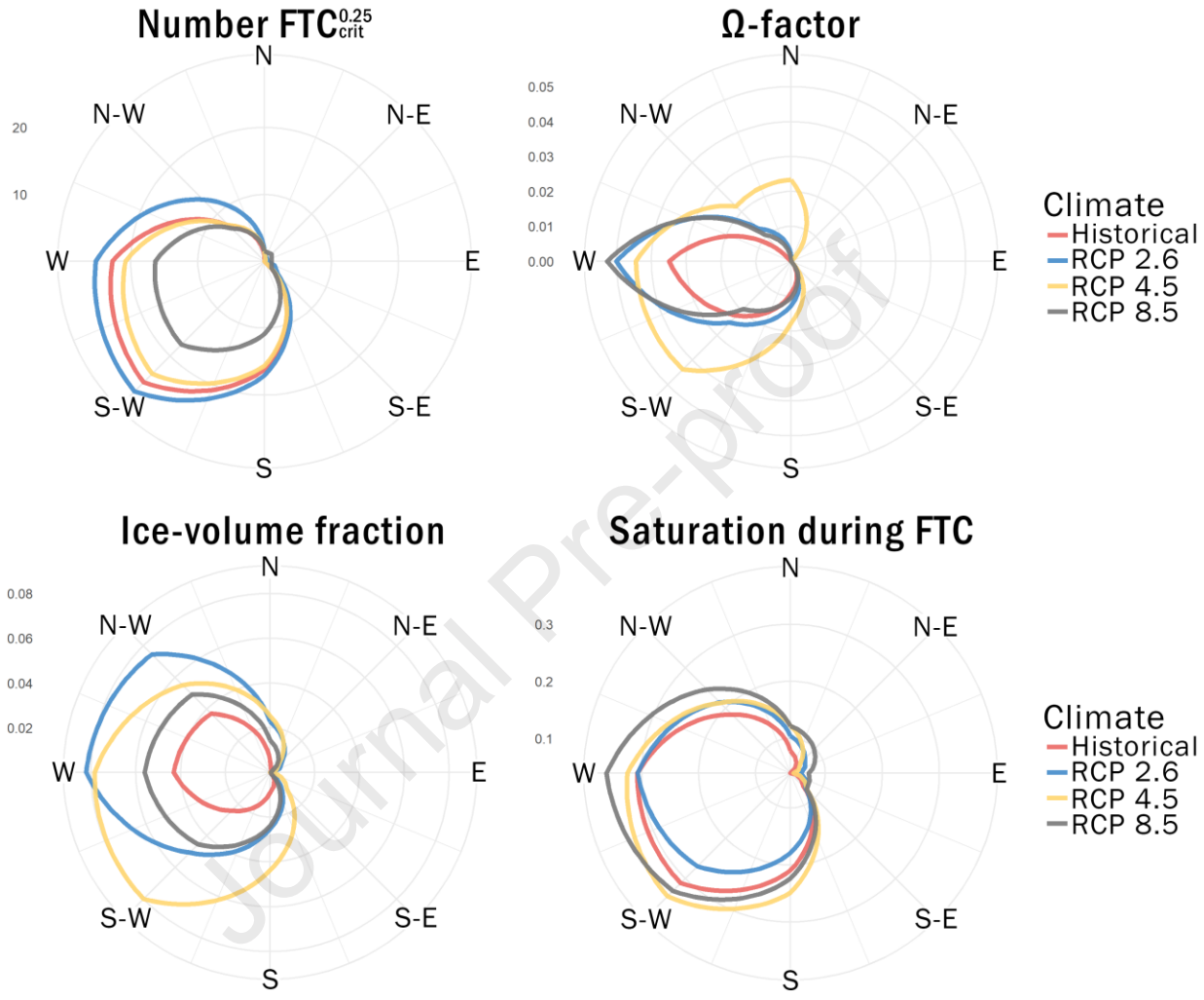

Figure 9. Orientation plot of the mean value of the number of $FTC^{0.25}_{crit}$, Ω-factor, the maximum ice-volume fraction during a FTC and the saturation during a FTC for the historical climate and the climate projections.

3.3 Towards a more representative method

Having established that both the material sensitivity methods as well as the $FTC_{crit}^{0.25}$ method are unreliable to assess frost damage risks, the following section provide a rationale for freeze-thaw assessment in future studies.

Finally, from this research, we would like to provide a framework to correctly assess the risk on frost damage for brick facades. Since not the same amount of resources and time are available for every study, the approach is divided into three options using the Superior, Advanced and Minimum requirement approach (SAMiRA) [42].

Superior: Fully characterize the hygrothermal material properties of the material at hand. Next, perform experimental frost tests of for different combinations of freezing temperatures and saturation degrees. After each cycle, measure the Ω-factor (and compare with visual observation of damage). Subsequently, run hygrothermal simulations with the characterised material properties and climate data to calculate the Ω-factor accordingly to assess the expected frost damage. (Material characterisation, experimental data and simulations)

Advanced: Material characterisation tests are deemed not available. Choose the best fitting material out of the material database of the simulation program to represent the bricks used in the experimental frost tests for different freezing temperatures and saturation degrees. Afterwards, run simulations with the correct climate data to calculate the Ω-factor accordingly to assess the expected frost damage. (Experimental data and simulations)

Minimum: The minimum requirement is only simulation based. Monitor the freezing temperature, saturation and ice-volume fraction whenever a FTC occurs. Use the classification charts in Figure 10. to select the Ω-factor for the frost cycles with the highest intensity.

The method applied in this research paper is an example of the Advanced method, since the materials of the experimental tests were not completely characterized, thus a representative material was chosen from the Delphin material database.

Since the experimental data of the original lab tests of Feng et al. [15] are not available, the classification tree in Figure 10 is developed. It combines the main conditions affecting the Ω-factor during a FTC: the freezing temperature (Temp), saturation degree (Saturation) and the ice-volume fraction (Ice-vol). The latter is important to include since this factor also contains information about the material characteristics and response. For instance, after simulations you encounter a FTC with 0.26 saturation going to -6°C with a ice-volume fraction of 0.13, than you count Ω=0.028 for that FTC. To obtain the total Ω-factor, you add the Ω for each cycle.

A classification tree provides more information than a Spearman rank correlation, because it is not a linear correlation model. At each step, the correlation is recalculated with all the parameters. The higher a parameter appears in the tree, the more significant it is. Noteworthy, as seen in Figure 10, very low freezing temperatures are often associated with moderate Ω-factors. This is because during a frost cycle with low freezing temperatures, saturation is lower since precipitation comes in the form of snow instead of rain, which is less absorbed by the materials.

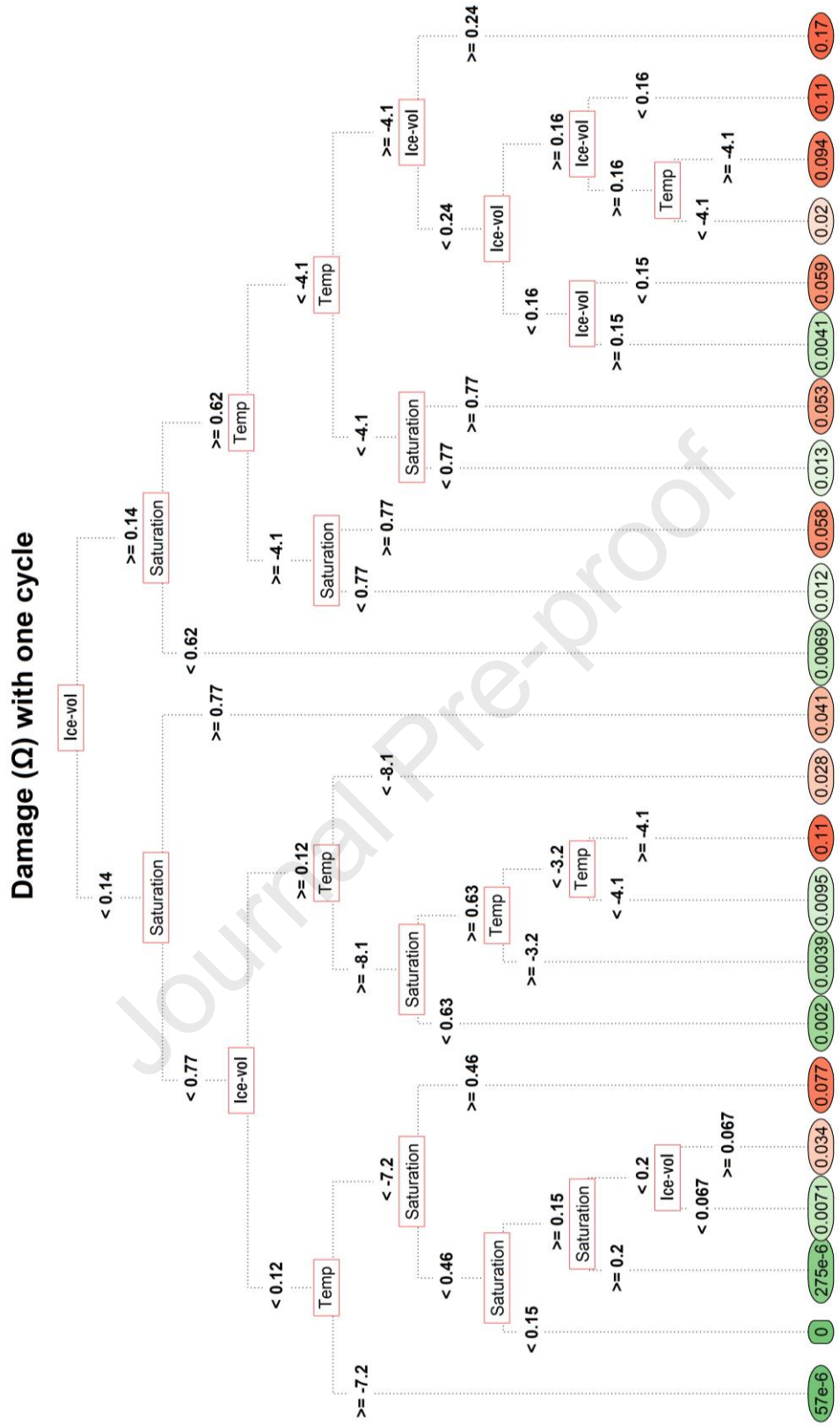

Figure 10. Classification tree of the expected Ω-factor during a FTC, with Ice-vol (ice-volume fraction), Temp (lowest freezing temperature during FTC) and Saturation (corresponding saturation degree)

The method is developed for brick material with a full saturation range (from 0 to 1) and a freezing temperature range from -20°C to 0°C. Please note, that the decision tree in Figure 10 is only applicable for a moderate climate, since it is specifically representative for the location of Brussels in Belgium.

4. Conclusions

This paper investigates different frost assessment methods. The different performance criteria were compared to the Ω-factor, derived from laboratory tests done by Feng et al. [15]. Hygrothermal simulations were performed to quantify the exposure-based methods. The following conclusions were drawn:

Firstly the material-sensitive criteria, the F_c-index and GC-factor, do not provide a trustworthy approach to determine whether a brick is frost sensitive or not. This is because the indexes only consider a limited number of material characteristics that do not sufficiently represent the material's pore structure and the related frost risk.

Secondly, counting the critical freeze-thaw cycles method based on Mensinga et al. (2010) [12] is also found not to be a reliable method for assessing frost decay. Even though the method entails similar trends with the boundary conditions compared to the Ω-factor, counting the number of $FTC_{crit}^{0.25}$ even has a negative correlation with the Ω-factor. Furthermore, changing S_{crit} for this frost assessment method does not entail any significant improvement because the results are very material dependent (and S_{crit} is not a parameter that is available or can easily be measured). A reason for the negative correlation between the number of $FTC_{crit}^{0.25}$ and the Ω-factor is related to the typical nature of real climate conditions. A high(er) number of freeze-

thaw cycles corresponds with lower saturation degrees during the FTC. Since the intensity of a frost cycle is more significant for damage than the number of cycles, it is more important to look into the conditions of the most extreme frost cycles than the number of low-threshold FTC's.

Finally, a workflow is presented to correctly assess frost decay risk. The Superior, Advanced and Minimum requirement approach (SAMiRA) is applied [42].

Superior: Fully characterize the hygrothermal material properties of the material at hand. Next, perform experimental frost tests for different combinations of freezing temperatures and saturation degrees. After each cycle, measure the Ω-factor). Subsequently, run hygrothermal simulations with the characterised material properties and climate data to calculate the Ω-factor accordingly to assess the expected frost damage.

Advanced: Material characterisation tests are not available. Select a representative material from the material database to represent the bricks used in the experimental frost tests for different freezing temperatures and saturation degrees. Afterwards, run simulations with the correct climate data to calculate the Ω-factor accordingly to assess the expected frost damage.

Minimum: The minimum requirement is only simulation based. Monitor the freezing temperature, saturation and ice-pore-percentage whenever a FTC occurs. Use the classification charts in Figure 10. to select the Ω-factor for the frost cycles with the highest intensity.

Finally, this paper illustrates the importance of selecting the appropriate methods when assessing freeze-thaw risks and showcases how different criteria diverge. Especially in climate change impact research, the choice of performance criterion can radically change the conclusion

on whether climate change will exacerbate or reduce a risk. Future research should study the Superior method for different wall set-ups to improve our understanding of frost damage and assess whether it is possible to find a threshold for the ice-volume fraction in a material to predict frost decay.

Nomenclature

Parameter	Description	Unit
A_{cap}	Capillary absorption coefficient	$kg/m^2s^{0.5}$
E	Elasticity moduli	Pa
F_c-index	Calculated frost resistance number	-
FTC	Freeze-thaw cycle	-
FTC_{crit}^{X}	Critical freeze-thaw cycle for a critical degree of moisture saturation X	-
GC-factor	Gélivité basée sur Capillarité factor	-
HAM	Heat-, Air- and Moisture	/
MRC	Moisture retention curve	/
p_{atm}	Atmospheric pressure	Pa
p_c	Capillary pressure	Pa
p_{crys}	Crystal pressure	Pa
p_l	Liquid pressure	Pa
PV	Pore volume per unit mass	m^3/kg
P3	Pore volume fraction for pores diameter larger than 3 µm	%
r	Pore radius of the smallest pore that freezes at temperature T	µm
RCP	Representative concentration pathway	/
R_v	Gas constant vapour	J/kgK
S_{crit}	Critical degree of moisture saturation	-
SAMiRA	Superior, Advanced and Minimum requirement approach	/
T	Temperature	K
t	Time	s
VCL	Vapour control layer	/
v_l	Specific volume liquid	$m^3/mole$
w_{cap}	Capillary moisture content	kg/m^3
w_{sat}	Saturated moisture content	kg/m^3
WDR	Wind driven rain	/
α	Contact angle	°
Δh_{ice}	Average molar heat of melting ice	J/mole
ΔS_{fv}	Entropy of fusion per unit volume of crystal	J/Km^3
γ_{vl}	Vapour-liquid interfacial energy	Jm^{-2}
γ_{il}	Ice-liquid interfacial energy	Jm^{-2}
φ	Relative humidity	-
ρ_l	Density of water	kg/m^3
Ω-factor	Relative change of the dynamic elasticity modulus	-

Acknowledgements

This work was funded by the Research Foundation Flanders (FWO), grant number 1S71922 and travel grant V463723N.

References

[1] C. Sabbioni, P. Brimblecombe, M. Cassar, and Noah's Ark (Project), *The atlas of climate change impact on European cultural heritage : scientific analysis and management strategies*. Anthem, 2010.

[2] X. Zhou, J. Carmeliet, and D. Derome, 'Assessment of risk of freeze-thaw damage in internally insulated masonry in a changing climate', *Build Environ*, vol. 175, May 2020, doi: 10.1016/j.buildenv.2020.106773.

[3] C. M. Grossi, P. Brimblecombe, and I. Harris, 'Predicting long term freeze-thaw risks on Europe built heritage and archaeological sites in a changing climate', *Science of the Total Environment*, vol. 377, no. 2–3, pp. 273–281, May 2007, doi: 10.1016/j.scitotenv.2007.02.014.

[4] O. Coussy and P. Monteiro, 'Unsaturated poroelasticity for crystallization in pores', *Comput. Geotech. 34*, pp. 279–290, 2007.

[5] M. Maage, 'Frost resistance and pore size distribution in bricks', *Matériaux et Construction*, vol. 17, no. 5, pp. 345–350, 1984, doi: 10.1007/BF02478706.

[6] D. Gerber, L. A. Wilen, F. Poydenot, E. R. Dufresne, and R. W. Style, 'Stress accumulation by confined ice in a temperature gradient', 2022, doi: 10.1073/pnas.

[7] S. S. L. Peppin and R. W. Style, 'The Physics of Frost Heave and Ice-Lens Growth', *Vadose Zone Journal*, vol. 12, no. 1, pp. 1–12, Feb. 2013, doi: 10.2136/vzj2012.0049.

[8] J. S. Wettlaufer and M. Grae Worster, 'Premelting Dynamics', 2005, doi: 10.1146/annurev.fluid.

[9] X. Zhou, D. Derome, and J. Carmeliet, 'Hygrothermal modeling and evaluation of freeze-thaw damage risk of masonry walls retrofitted with internal insulation', *Build Environ*, vol. 125, pp. 285–298, Nov. 2017, doi: 10.1016/j.buildenv.2017.08.001.

[10] G. Fagerlund, 'The critical degree of saturation method of assessing the freeze/thaw resistance of concrete.', prepared on behalf of RILEM Committee 4.

[11] A. Prick, 'Critical degree of saturation as a threshold moisture level in frost weathering of limestones', *Permafr Periglac Process*, vol. 8, no. 1, pp. 91–99, 1997, doi: 10.1002/(SICI)1099-1530(199701)8:1<91::AID-PPP238>3.0.CO;2-4.

[12] P. Mensinga, J. Straube, and C. Schumacker, 'Assessing the freeze-thaw resistance of clay brick for interior insulation retrofit projects', 2010. [Online]. Available: https://www.researchgate.net/publication/288364222

[13] K. Calle, 'Renovatie van historische gevels: redding of doodsteek? Renovation of Historical Facades: The Rescue or the Kiss of Death?', 2020.

[14] 'NBN B 27-009/A2: Ceramic products for wall and floor covering - Frostresistance - Freezing and thawing cycles', 1996.

[15] C. Feng, S. Roels, and H. Janssen, 'Towards a more representative assessment of frost damage to porous building materials', *Build Environ*, vol. 164, Oct. 2019, doi: 10.1016/j.buildenv.2019.106343.

[16] F. Radjy, 'Kompendium i bygningsmateriallaere, theoretisk del. Laboratoriet for Bygningsmaterialer', *DTH. Danish.*, 1971.

[17] O. Coussy and P. J. M. Monteiro, 'Poroelastic model for concrete exposed to freezing temperatures', *Cem Concr Res*, vol. 38, no. 1, pp. 40–48, 2008, doi: 10.1016/j.cemconres.2007.06.006.

[18] F. T. Wall, *Chemical Thermodynamics*. San Francisco, 1965.

[19] S. C. Hardy, 'A grain boundary groove measurement of the surface tension between ice and water', *Philosophical Magazine*, vol. 35, no. 2, pp. 471–484, Feb. 1977, doi: 10.1080/14786437708237066.

[20] E. Vereecken, 'Hygrothermal Analysis of Interior Insulation for Renovation Projects', 2013.

[21] M. Prignon, T. De Mets, E. Vereecken, and A. Tilmans, 'Frost Damage Risk in Insulated Masonry Walls: Challenges in Analysing Large Number of Numerical Simulations'.

[22] G. Berghmans, T. De Kock, G. De Schutter, and V. Cnudde, 'Evaluatie van vorstschade bij kalkstenen: een technische beoordeling', 2012.

[23] 'NBN B 27-010: Keramische produkten voor wand- en vloerbekleding - Vorstbestendigheid - Vermogen tot wateropslorping door capillariteit', 1983.

[24] M. Dusar, R. Dreesen, and A. F. De Naeyer, *Renovatie & restauratie: natuursteen in Vlaanderen, versteend verleden*. Mechelen: Wolters Kluwer, 2009.

[25] H. Janssen, C. Feng, and S. Roels, 'Impact of frost temperature and moisture content on frost damage to ceramic bricks', doi: 10.1051/matecconf/201928.

[26] 'BS EN 12371 2010 Natural stone test methods -Determination of frost resistance.'.

[27] A. Al-Omari, K. Beck, X. Brunetaud, Á. Török, and M. Al-Mukhtar, 'Critical degree of saturation: A control factor of freeze-thaw damage of porous limestones at Castle of Chambord, France', *Eng Geol*, vol. 185, pp. 71–80, Feb. 2015, doi: 10.1016/j.enggeo.2014.11.018.

[28] G. Fagerlund, 'Fatigue effects associated with freeze-thaw of materials', 2000.

[29] A. Nicolai and J. Grunewald, 'Delphin 5 User Manual and Program Reference', 2003.

[30] J. Wei, S. Yu, and X. Zhou, 'Study on influence of geometric characteristics of cracks on HAM coupling transfer and thermal performance of multi-layer cellular concrete wall', *J Build Phys*, p. 174425912211219, Nov. 2022, doi: 10.1177/17442591221121918.

[31] C. Feng and H. Janssen, 'Hygric properties of porous building materials (VII): Full-range benchmark characterizations of three materials', *Build Environ*, vol. 195, May 2021, doi: 10.1016/j.buildenv.2021.107727.

[32] J. Zhao, 'Development of a Novel Statistical Method and Procedure for Material Characterization and a Probabilistic Approach to Assessing the Hygrothermal Performance of Building Enclosure Assemblies', 2012.

[33] O. Giot *et al.*, 'Validation of the ALARO-0 model within the EURO-CORDEX framework', *Geosci Model Dev*, vol. 9, no. 3, pp. 1143–1152, Mar. 2016, doi: 10.5194/gmd-9-1143-2016.

[34] J. Leissner *et al.*, 'Climate for culture: Assessing the impact of climate change on the future indoor climate in historic buildings using simulations', *Herit Sci*, vol. 3, no. 1, 2015, doi: 10.1186/s40494-015-0067-9.

[35] I. Vandemeulebroucke, N. Van Den Bossche, and S. Caluwaerts, 'Untangled: Climate Projections for Hygrothermal Modelling of Building Envelopes.', 2023.

[36] 'CEN. EN ISO 6946. Building Components and Building Elements—Thermal Resistance and Thermal Transmittance—Calculation Methods; CEN: Brussels, Belgium, 2017.'

[37] 'CEN. EN ISO 15927-3. Hygrothermal performance of buildings—Calculation and presentation of climatic data—Part 3: Calculation of a Driving Rain Index for Vertical Surfaces from Hourly Wind and Rain Data; CEN: Brussels, Belgium, 2009'.

[38] K. Calle and N. Van Den Bossche, 'Sensitivity analysis of the hygrothermal behaviour of homogeneous masonry constructions: Interior insulation, rainwater infiltration and hydrophobic treatment', *J Build Phys*, vol. 44, no. 6, pp. 510–538, May 2021, doi: 10.1177/17442591211009937.

[39] ‘Faculty of Architecture Institute for Building Climatology Building Physics DELPHIN Course’.

[40] K. Janssens, V. Marincioni, N. Van, and D. Bossche, ‘Improving hygrothermal risk assessment tools for brick walls in a changing climate’.

[41] I. Vandemeulebroucke, S. Caluwaerts, and N. Van Den Bossche, ‘Factorial study on the impact of climate change on freeze-thaw damage, mould growth and wood decay in solid masonry walls in Brussels’, *Buildings*, vol. 11, no. 3, Mar. 2021, doi: 10.3390/buildings11030134.

[42] B. Vanderschelden, M. A. Lacasse, T. Moore, N. Van, and D. Bossche, ‘Methodological framework for HAM-simulations: the litigation case of a CLT-balcony subjected to rain loads during construction’.

Highlights:

- Assess frost risk with response-based methods, not material sensitivity methods
- Hygrothermal simulations provide relevant insights on frost damage understanding
- Various frost assessment methods yield diverse climate response outcomes
- More freeze-thaw cycles do not necessarily result in higher frost damage
- Offering a time-resource dependent framework for accurate frost damage assessment

Declaration of interests

☒ The authors declare that they have no known competing financial interests or personal relationships that could have appeared to influence the work reported in this paper.

☐ The authors declare the following financial interests/personal relationships which may be considered as potential competing interests: